Department of Information Technology and Mathematical Methods

Working Paper

Series "*Mathematics and Statistics*"

Multivariate hierarchical statistical detectors for

health surveillance and diagnostics with example

of a cable stayed bridge

by

Alessandro Fassò

Multivariate hierarchical statistical detectors for health surveillance and diagnostics with example of a cable stayed bridge

Alessandro Fassò

University of Bergamo,
Dept. of Information Technology and Mathematical Methods
Via Marconi 5, 24044 Dalmine BG, Italy
alessandro.fasso@unibg.it

December 2009

1 Introduction

Modern monitoring systems are usually intended to ensure safety surveillance and maintenance supervision of concrete structures and bridges which are often equipped with a number of instruments and sensors. Meanwhile, techniques for optimal design and dimensioning under budget constraints are being studied in this field, there is a tendency to have highly instrumented monitoring systems, with sensors for example for each bridge pier, joint, cable etc.. Moreover, low frequency monitoring systems, based e.g. on hourly data, are more common in actual field monitoring as they involve a reduced amount of data and, correspondingly, relevant savings in data communication, computation and storage. Although, high frequency measuring systems are promisingly being studied for structural health monitoring based on modal vibration analysis and classification, see e.g. Basseville et al. (2004 and 2007) and Carden & Brownjohn (2008), they are not widespread because of high costs and because the same authors show some evidence that classification methods based on dynamic parameters give pour results.

Since visual inspection of such data is inadequate, methods for data analysis and decision making are called for. Hence, this paper after reviewing statistical monitoring iun general, proposes a method able to extract information from a possibly complex monitoring system for medium and long term bridge surveillance through sequential structural health assessment. In particular, the proposed method is illustrated with reference to the Certosa cable-stayed bridge in Milan, Italy, which is presented in section 2 and discussed in more details by Biondini et al. (2006a, b) and Bruzzi et al. (2007).

After introducing the general concept of statistical monitoring and sourveillance in section 4, sections 3 and 5 introduce the two blocks which are skeletonized in Fig. 1 and constitute the statistical surveillance system. At the first stage, a statistical

monitoring system model (MSM) is used for understanding the bridge dynamics under normal conditions. This implies dynamical modeling and adjustment for all the observed external forcing factors, the main being temperature (see e.g. Wah, 1971) then wind and traffic load. As a modeling by-product, the first stage gives also the estimated correlation structure of the stochastic errors involved which describe both the measuring and the modeling errors and are important, not only for understanding the uncertainty reduction given by the MSM, but also for defining the optimal multivariate detector.

The second block is a multivariate hierarchical detector (MHD), which is applied to the output of the previous MSM and gives, as a first output, a single value global health statistics which is compared on line with an upper threshold. In case of exceedance, a first level signal is given and a decision tree is used to localize the source of the event according to a previously defined monitoring system segmentation based on structural or instrumental criteria. Section 6 illustrates the performance of the surveillance system on the basis of some artificial anomalies applied to Certosa bridge data.

2   The monitoring data

The motivating example is based on the cable-stayed bridge over the Milan-Certosa railway-junction, which was erected in 1980's and is depicted in Fig. 2. After the structural rehabilitation, whose lifetime impact has been discussed in details by Biondini et al. (2006b), a number of new instruments have been installed including jointmeters (JM), deflection meters, clinometers (CL), and thermometers, which complement the data of the previously installed load cells (LC). For example, the four pylons have been equipped with two-directional clinometers, jointmeters have been fixed at the base of the deck, while deflection meters have been installed at the center of two spans of the bridge for measuring the vertical movements.

Although the bridge is presently equipped with more then thirty instruments, only those which yielded good data for long enough time have been used in this study. In particular, in order to have sufficient data for both model identification and validation, the period from April 1, 2005 to January 10, 2007 has been considered with three time series for clinometers, five for jointmeters, five for load cells and four for temperature. Figure 3, shows the different, scales, trends and behaviors for the corresponding instruments; moreover the validation dataset, in black ink, begins April 8, 2006.

On the one side, as shown by Tab. 1, the jointmeters are strongly correlated with temperature, whilst clinometers are not correlated nor with temperature nor with the other instruments and behave erratically like white noises processes as shown by the analysis of the autocorrelation function performed by Bruzzi et Al. (2007). The load cells have an intermediate behavior with some inertia and some correlation with the jointmeters but without the clear seasonal trend shown by the jointmeters.
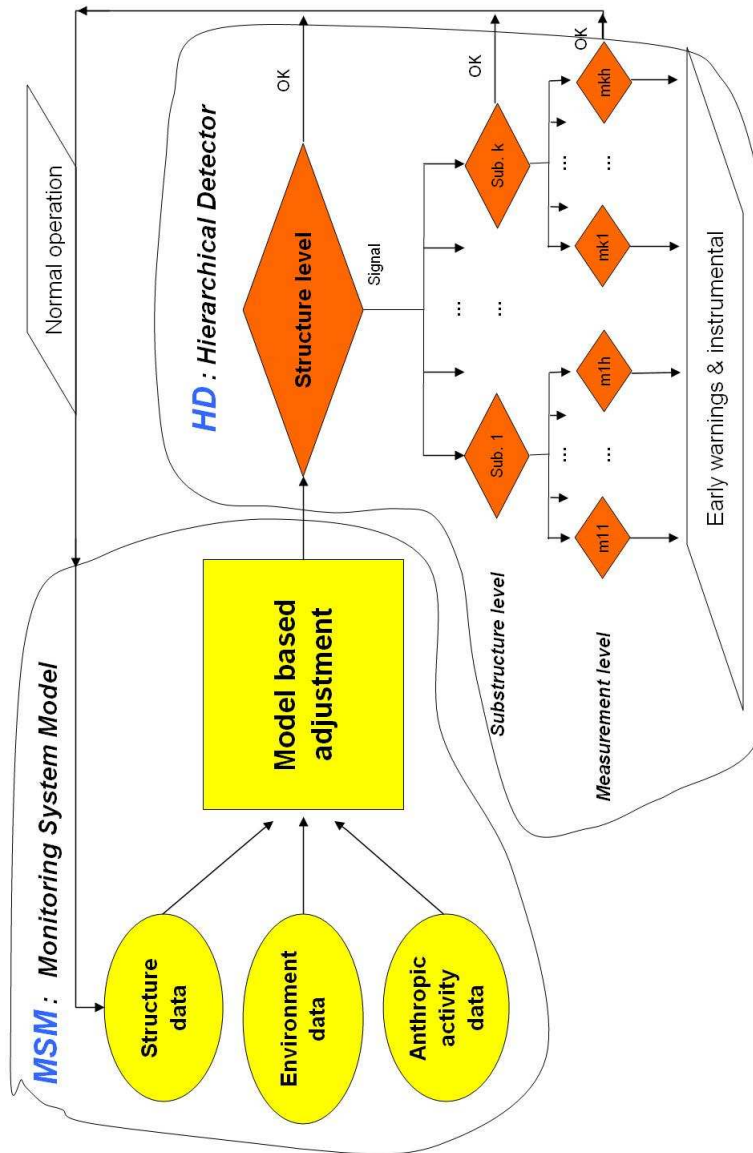
Figure 1: Skeleton for monitoring system model (MSM) and connected hierarchical detector model (HDM).

Figure 2: Milan-Certosa bridge

	Clinometers	Jointmeters	Load cells
Clinometers	low	low	low
Jointmeters		High $(+)$	Medium $(-)$
Load cells			Medium $(+)$

Table 1: Synoptic correlation matrix for Certosa sensors.

3   The monitoring system model

The first of the two blocks underlying the surveillance system of Fig. 1 is a model for the monitoring system (MSM) intended as a unique multivariate process subject to the forcing factors related to normal functioning. This is aimed at understanding the behavior and dynamics of the monitoring system through statistical correlations, which are able to assess the structural relationships among the bridge components and their response to environmental and anthropic factors.

According to this, the set of structural measurements at time t, denoted by y_t, is related to the set of external covariates, denoted by x_t, through a measurement error, e_t, and a dynamical component, μ_t, which is not directly observed. Hence the MSM is given by the following set of vector equations,

$$
\begin{aligned}
y_t &= \mu_t + e_t \\
\mu_t &= Dx_t + \eta_t \\
\eta_t &= A\eta_{t-1} + \varepsilon_t
\end{aligned} \tag{1}
$$

The first one is an observation equation where the measurement error e_t is a multivariate Gaussian white noise with covariance matrix denoted by R, which takes into account the structural relationships after adjusting for thermal effects and time dynamics.

The second equation in (1) describes the underlying MSM dynamics as the sum of an observed component and a colored noise denoted by η_t. In particular, the matrix D explains the effect of the external factors on the system. In this paper, the nonlinear thermal effect is described by five different components given by the long term high temperature, the long term low temperature and the short term
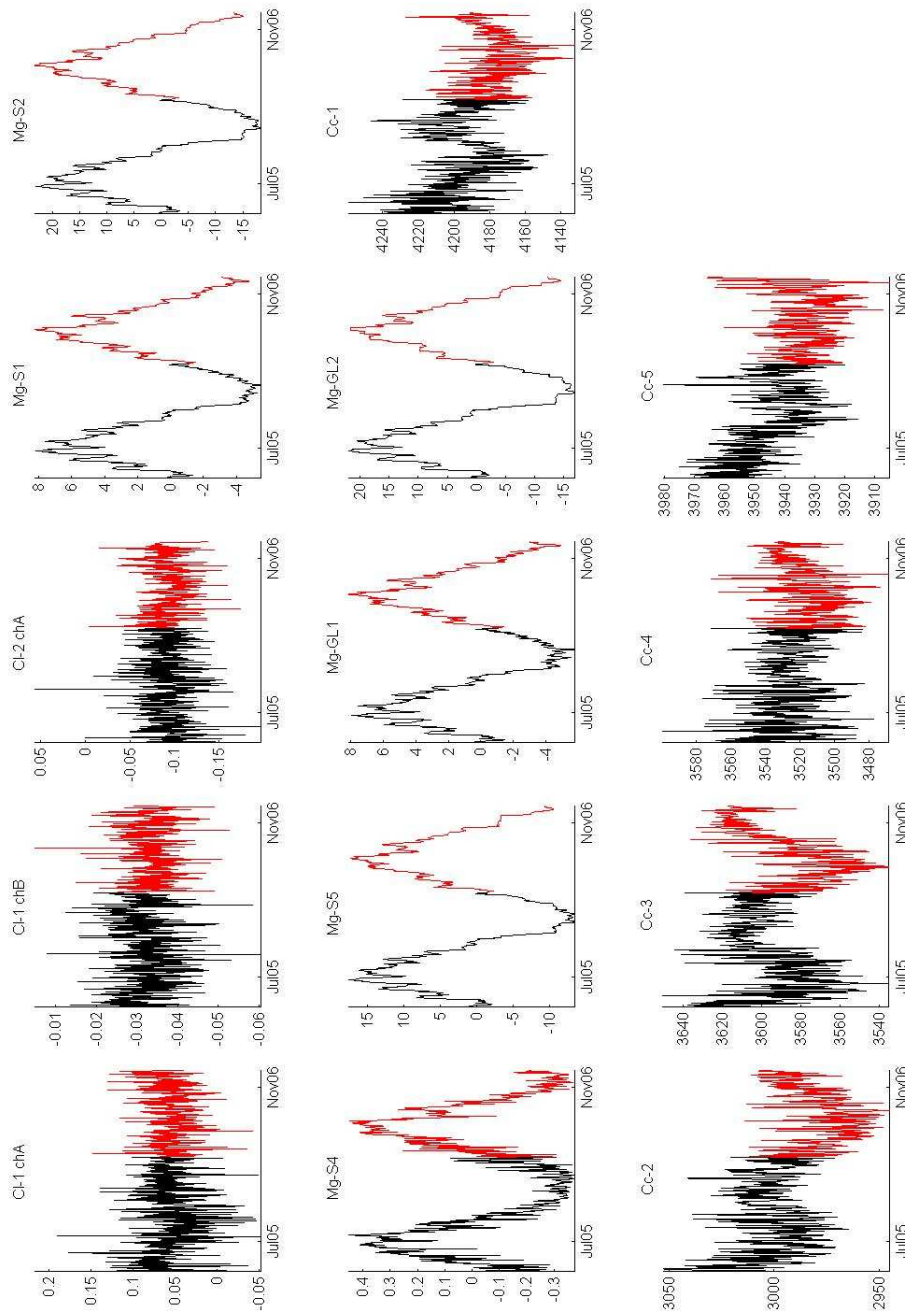
4

Figure 3: Time series for the following instruments: clinometer, CL-prefix, sexadecimal degrees; jointmeter, JM-prefix, mm; load cell, LC-prefix, kN, thermometer, T-prefix, °C. Estimation dataset is the black part, from April 1, 2005 to April 7, 2006. Validation dataset is the remaining red part.

variation of Fig. 4, together with the delayed effects of one and two days for the short term temperature variation. Note that the two long term effects have been computed as a 30 days temperature moving average cut, respectively, below and above the median and the short term effect is simply the error term of the above moving average.
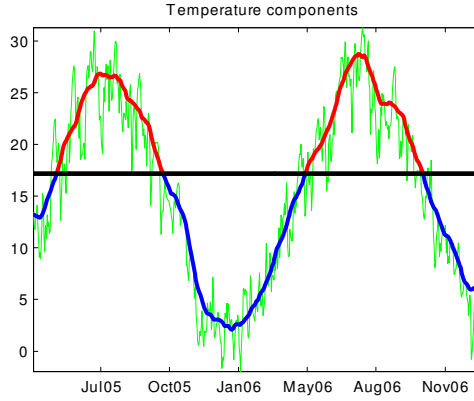

Figure 4: Non symmetric thermal effect with temperature (°C) from T-S1: red is long term high temepature, blue is long term low temepature and green is short term variation.

Moreover, the persistency of the unobserved dynamic component,, is given by the propagation matrix A, which has nonzero elements only on the main diagonal. Similarly to the error, also the innovation is supposed multivariate Gaussian white noise with covariance matrix given by $\Sigma = KRK'$, where the squared matrix K is related to the so called Kalman gain. Of course the introduced noises take into account the reduced information on the monitoring system and, hence, estimates of A, Σ and R are useful for fair uncertainty assessment. In this paper the three equation of model (1) have the same dimension, which is thirteen for Certosa monitoring system.

3.1 Partitioning

In some cases, it may be convenient to segment the monitoring system and the observation set into blocks according to a structural or instrumental criterion. For example Certosa bridge MSM may be partitioned according to the three types of instruments installed, say A for clinometers, B for jointmeters and C for load cells, which gives

$$y = (y_A, y_B, y_C)$$

and $e = (e_A, e_B, e_C)$ is conformably partitioned. Accordingly, the covariance matrix of e_A is R_A and similarly for e_B and e_C. In the contest of partitioned systems, an MSM is said to be a block diagonal monitoring system model if K is a block diagonal matrix. This gives a block diagonal innovation model as the varaince covariance matrix Σ satisfies the block diagonal property which is useful for simplifying anomaly localization of section 5.

3.2 Model estimation

Following standard practice (see e.g. Ljung, 1999), the model identification and minimum prevision error estimation of model (1) has been based on the first year of available data after removing the averages and rescaling to unit variance each measurement component. Then, using the Akaike criterion known as AIC, only the coefficients having a Student's t statistic larger then the threshold 1.8 were included in the final model. The corresponding estimates for D and A, are reported in Tab. 2 together with the respective standard deviations which are quite small and confirm the limited uncertainty and good quality of these estimates.

Confirming the expectations based on preliminary analysis, the elements corresponding to the clinometers are taken as zero by above AIC criterion, both in D and A, and no uncertainty reduction is given for these instruments. Nevertheless keeping these components in the model is useful for the multivariate detection approach of section 5.

	Estimated coefficients					Standard deviations				
	Const	Heat	Cold	Short	A	Const	Heat	Cold	Short	A
Cl-1 chA	1.55					.056				
Cl-1 chB	-4.11					.055				
Cl-2 chA	-3.23					.054				
Jm-S1	0.38	0.45	0.63	0.10	0.83	.034	.020	.020	.004	.02
Jm-S2	0.38	0.41	0.68	0.07	0.89	.038	.021	.021	.004	.01
Jm-S4	-0.38	0.59	0.38	0.21	0.83	.118	.064	.063	.022	.02
Jm-S5	0.41	0.40	0.68	0.08	0.88	.034	.019	.019	.004	.01
Jm-GL1	0.37	0.45	0.62	0.12	0.79	.025	.015	.015	.004	.02
Jm-GL2	0.44	0.40	0.69	0.05	0.90	.049	.027	.027	.004	.01
Lc-1	219.1			-0.55	0.96	.721			.056	.01
Lc-2	181.0	-0.47		-0.76	0.90	.364	.149		0.05	.02
Lc-3	179.4			-0.66	0.97	.941			.050	.01
Lc-4	189.1			-0.72	0.97	1.11			.067	.01
Lc-5	337.2			-0.29	0.87	.253			.059	.02

Table 2: Estimates of model coefficients for matrices D and A with estimation uncertainties.

On the other side, for jointmeters and load cells, which have non trivial D coefficients, the propagation coefficients from matrix A entail an important stable dynamics after thermal adjustment as the minimum of the diagonal of matrix is 0.807 (with standard error 0.028) and the maximum is 0.957 (with standard deviation 0.011). Moreover, the two seasonal effects assessed by the coefficients of matrix D related to long term high temperature and long term low were significantly different, confirming asimmetry and the above idea of separating summer and winter thermal effects.

The single figures for the remaining estimated coefficients in K and R are omitted here for brevity. Just note that the covariance matrix R shows strong correlations among the load cells, medium correlations among the jointmeters and low among

the inclinometers. Also the cross correlations among different instruments are fairly low being generally less than 0.25 and close to zero for the clinometers. Comparing to the synoptical correlation of Tab. 1 shows that the raw data correlations are different from correlations adjusted for thermal effect and time dynamics.

It is worth observing that the fitted model explains the large part of the normal variability of jointmeters as the five residual variances are less than 0.2% of the total measurement variance. This fitting reduced but still interesting for the load cells as the residual variances are now less then 43% of the corresponding total variances. For the clinometers, as mentioned above, no reduction is given but, nevertheless, embedding these measurements into the MSM is useful for the subsequent analysis.

The validation process has been carried out on two different steps. At the first, the estimated model (1) has been checked for the so called in-sample residual analysis, which confirmed, on the basis of graphical tests applied to the estimation dataset, the hypothesis of normality and white noise for the errors et. The second and more fundamental validation step is based on assessing the properties of the overall surveillance system working on the second year data as in sections 6.

4   Statistical surveillance excursus

Statistical surveillance has its historical roots in the $1920's$ for quality control applications with the celebrated Shewhart's control chart. At that time Walter A. Shewhart, working at Western Electric and Bell Telephone Laboratories, proposed a simple control chart for controlling manufacturing process and enabling to distinguish between common-causes (or in-control) and assignable-causes (or out-of-control). See e.g. Bayart (2001) and Shewhart (1931).

Fig. 5 shows a reinterpretation of the original proposal, where daily deviation from the in-control target, say y_t, is plotted against time. The central line corresponds to the expected level when the process is in-control, taken as zero in the example used here, and the two dashed lines at ± 3 times the common-causes standard deviation ($\sigma = 0.1$) define the rule which signals for an assignable-cause.

From both the practical and theoretical point of view, this approach has a neat interpretation if the process measurements are independent on different days and Gaussian distributed in the absence of anomalies. Under these assumptions, in the long run, it gives a rate of false positives which is 0.27% and the mean time between false positives, which is known as the in-control Average Run Length, is 370 days, or $ARL(0) \cong 370$. These figures can be tuned to special needs by moving the above thresholds from $\pm 3\sigma$ to the appropriate percentiles.

If an "assignable cause" is in act causing a shift of the process mean then, the time to detection is expected to be correspondingly reduced. For example if the true process level is $\Delta = 2\sigma$ instead of zero, then the average time to detection is $ARL(2\sigma) \cong 6.3$ but for smaller deviations, e.g. $\Delta = \sigma$, a longer time to detection is implied, namely $ARL(\sigma) \cong 44$.

Referring back to bridge slab data of section 2, Fig. 6 shows control charts for the clinometric readings which are independent of time. The left panel shows one-year observed data with no anomalies and one isolated false warning at day 117. The right panel is related to a simulated anomaly which has been obtained by adding to
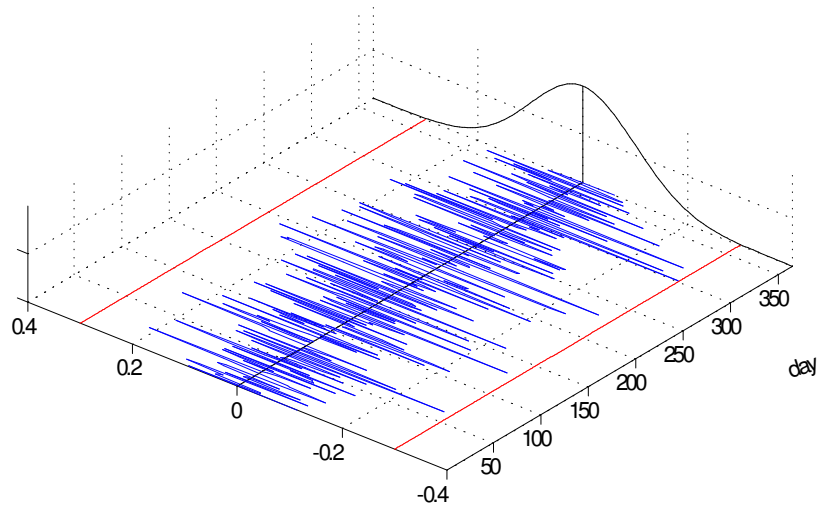
Figure 5: One year data for a Shewhart control chart with superimposed parent Gaussian distribution.

the observed data of left panel and additive anomaly which starts at day 167 and gradually rise to 1σ. It is apparent that it is hardly recognized by the $\pm 3\sigma$ Shewhart control chart.
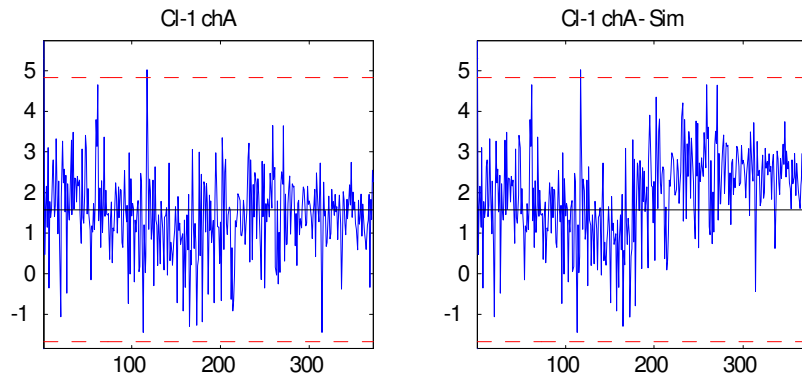

Figure 6: Shewhart control chart for clinometer data. Abscissa: day. Dashed lines: $\pm 3\sigma$ bands. Left panel: observed data. Right panel: observed plus simulated anomaly of size 1σ and transient from 167th day.

4.1   Accumulating information over time

Since Shewhart, control charts have been extensively studied, modified and extended to cover a huge variety of new situations which arise from the massive use of automatic data collection in many areas and the related need to have automatic and objective criteria to implement surveillance, see e.g. Montgomery (2005).

9

From the application point of view, many new fields have been devised, for example: computer intrusion detection based on event intensity occurring in the information system to be sheltered (see e.g. Ye et al., 2002); financial portfolio monitoring (Golosnoy and Schmid, 2007); epidemiological surveillance based on counts control charts where y_t is the count of morbidity events (Woodall, 2006).

From the method point of view, the basic approach of Shewhart is recognized to be a change detector without memory as, at each time t, it uses only the present data y_t without reference to the past history of y_t itself. It is then tailored for detecting large abrupt changes in data which does not show periodic fluctuations and inertia. The first fundamental line of extension is then related to give more efficiency in change detection by means of reducing the delay time, especially for small changes.

Suppose a permanent step change or assignable-cause takes place at time t^* and this is of size $\Delta \neq 0$ on average, namely $E(y_t) = \Delta$. The detection time $\hat{t}$ and delay $\hat{t} - t^*$ are then of interest. Under the afore mentioned Shewhart assumptions the expected time to detection, $E_\Delta(\hat{t} - t^* + 1)$ or Average Run Length under Δ is the reciprocal of the probability of an exceedance, that is

$$ARL(\Delta) = \frac{1}{P_\Delta(|y_t| > 3\sigma)}. \tag{2}$$

This quantity is to be reduced by accumulating information over time. To do this a simple and effective way is smoothing the data by an exponentially weighted moving average ($EWMA$), namely

$$z_t = \lambda y_t + (1 - \lambda) z_{t-1} \tag{3}$$

with a small positive smoothing factor λ, formally $0 < \lambda < 1$, which can be chosen to optimize the average detection delay for certain fixed change amplitudes. As deviations are being considered from a reference value, the $EWMA$ detector gives a warning if

$$|z_t| > h$$

where the symmetric threshold h is determined in order to control the false signal probability. Although the threshold h still retains the interpretation in terms of false positive probability as for the Shewhart control chart, equation (2) does not hold in such a simple form and the ARL computation requires numerical methods which may be based on Markov chains methodology in simple cases (see e.g. Runger and Prabhu, 1996) and on the Monte Carlo and/or Bootstrap methods for more complicated ones (see e.g. Fassò ad Locatelli, 2007).

Considering the same clinometric anomaly of Fig. 6, the following Fig. 7 definitely shows that smoothing is effective for signalling small changes.

Alternative techniques for accumulating past information (Basseville and Nikiforov, 1993) are based on the $CUSUM$ statistic and maximum likelihood ratio's. Extensive applied and numerical analysis showed that, these three approaches are very close one each other and $EWMA$ is actually the preferred one among practitioners and statisticians because is flexible and simple.

4.2   Multivariate control charts

The second fundamental line of extension is related to the complexity of measurement set y_t. Taking into account that y_t is a measurement set of correlated quantities
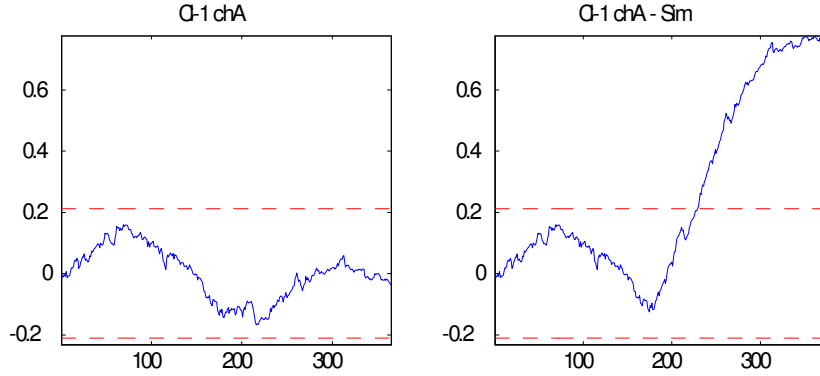
Figure 7: EWMA control chart for clinometer data. Abscissa: day. Dashed lines: $\pm 3\sigma$ bands. Left panel: observed data. Right panel: observed plus simulated anomaly of size 1.5σ and transient from 167th day. Smoothing $\lambda = 0.01$.

(Fuchs and Kennet, 1998), joint monitoring all the averages together can be done by multivariate $EWMA$ charts (Bersimis et al., 2006, Lowry et al., 1992). The basic idea is to use a statistic which takes into account correlation among the components of y_t. Under the assumption that the measurement set y_t is multivariate Gaussian, such a quantity is the squared Mahalanobis distance from the target here assumed to be zero, namely

$$X_t^2 = z_t \Sigma^{-1} z_t \tag{4}$$

where Σ^{-1} is the inverse of the variance-covariance matrix of z_t, which is given by the vector counterpart of recursive equation (3). After an overall change is signalled by the exceedance of an appropriate threshold, namely

$$X_t^2 > h,$$

the diagnostic problem of identifying the particular measurement subsets which are responsible for the detection has to be addressed.

Note that X^2 of equation (4) is constant for all $z's$ laying on the contour of the corresponding multivariate Gaussian distribution. For example Fig. 8 shows the bivariate case with correlation $\rho = 0.8$, where $z's$ along the bisector of the first and third quadrant are more common under normal operations and, conversely, the statistic is larger in the opposite direction which is very uncommon under normal operations and therefore is to be interpreted as stronger evidence of assignable causes.

5   The hierarchical multivariate detector

In this section the multivariate control chart technique is hierarchically applied to various subsets of the outputs from MSM.

In particular surveillance is based on filtered data, namely on the residual e_t, computed day by day, using the estimated version of model (1). In order to have a decision tree procedure, which strongly controls the overall false detection rate
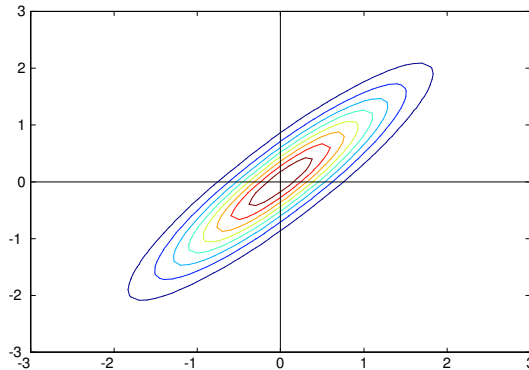
11

Figure 8: Contours of the bivariate Gaussian distribution with correlation $\rho = 0.8$.

(see e.g. Fassò, 1992, and Hochberg & Tamhane, 1987), the residuals are fed to a hierarchical multivariate detector (HMD) through a multivariate exponentially weighted moving average of the previous section.

The first step, is applying the vector recursion of equation (3) to the residuals, where the smoothing parameter λ taken as a scalar here, but, generally speaking, may be a matrix enabling to have different smoothing for the different model components. Then, the stability of the whole structure is summarized by the single value statistic (4).

In case the MSM is a block diagonal system, as approximately holds for the Certosa MSM, equation (4) can be decomposed into the sum of the corresponding second level statistics, namely:

$$X_t^2 = X_{A,t}^2 + X_{B,t}^2 + X_{C,t}^2 \tag{5}$$

The statistic X_t^2 may be plotted against t with small values are related to global structural normality. On the other side, if some structural properties change or some instruments fail, than persistently large values of X_t^2 are expected.

To be more precise, the procedure which gives a signal at time t if

$$X_t^2 > h$$

is defined the first level detector. When such a first level signal is given, then the second level detectors are activated for blocks $S = A, B$ or C. When

$$X_{S,t}^2 > h_S$$

then the second level detectors give a signal at block S and the corresponding third level detectors are activated. This gives a signal at instrument j of block S when

$$z_{j,t}^2 > h_j$$

Note that, the case of three levels and three blocks considered in this paper can be straightforwardly extended to more general setups, allowing for mixed strategies partly related to structural criteria (bridge pylons, deck etc.) and partly to instrumental criteria.

5.1 Estimation of thresholds

In order to use the proposed hierarchical procedure for detecting and localizing structural anomalies as discussed in the next section, the above thresholds have been estimated for a false detection probability of 0.001 and using a computer intensive approach. In particular, these quantities have been computed as percentiles of the gamma distributions approximating the stationary distributions of , and of its sub-components, which have been obtained by 10'000 days long simulated time series. Each time series has been simulated using model (1). To do this, first the covariates have been simulated by an extension of the block bootstrap used by Fassò & Locatelli (2007) with an average block length of 60 days and with each block randomly amplified by a stochastic factor which increases the meteorological uncertainty.

For taking into account the uncertainty of the estimates from section 3, the 95% worst case approach of Aply & Lee (2005) has been considered empirically. In particular, the previous simulations have been replicated 200 times. At each replication, the generating model coefficients have been randomly generated from the multivariate Gaussian distribution describing the uncertainty of to the estimates of section 3 in large samples.

6 Case studies

In order to study the properties of the MHD a number of simulation studies have been considered, see Bruzzi et al. (2007) and Fassò and Pezzetti (2007) for more details. Here, for illustrating its use and behavior, the validation dataset starting on April 8, 2006 is considered as in Section 2 and Figure 3. The $EWMA$ detectors of previous section have been implemented with a smoothing factor $\lambda = 0.1$, which is appropriate for detecting medium to small anomalies.

The first example considers an artificial anomaly at the joint in the southern end of the bridge deck. Fig. 9 shows the observed and corrupted data for jointmeters S2 and GL2. The simulated anomaly is given by two additive transients with opposite sign, which start at August 1st, 2006, or the 500th day, and linearly reach $\pm 6mm$ in two months. The anomaly size is quite small with respect to the total standard deviations which are $12.08mm$ and $11.54mm$ for JM-S2 and JM-GL2, respectively. Correspondingly, Figure 10.a shows that the first level detector gives a signal at day 515, which is an early detection and is much more clear than single measurements inspection. After the first level warning, the second level detectors have to be checked for threshold exceedances. The remaining three panels of Figure 10 show that the cause of the first level signal is localized at the jointmeters block. As expected, the third level detectors of Figure 11 clearly idenitify the most probable sources of the anomaly at jointmeters S2 and GL2, where permanent thresholds exceedances start around day 530.

The second example shows that for those instruments where no uncertainty reduction is achieved at the MSM step only those deviations which are larger in a statistical sense, may be detected.
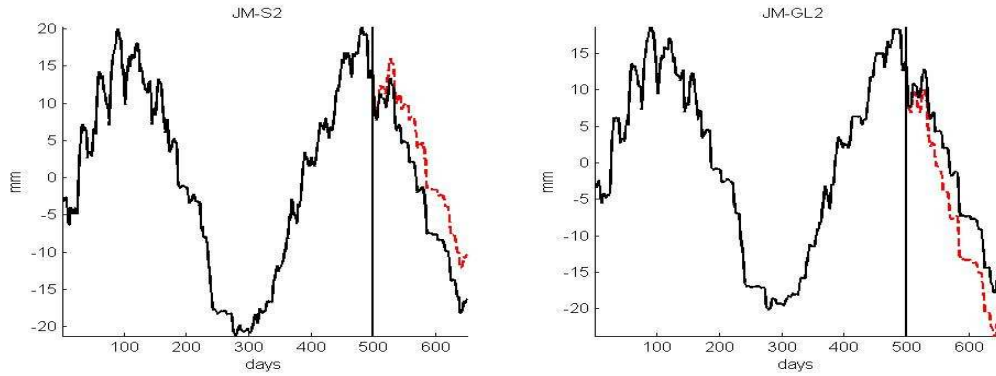
Figure 9: Southern end deck joints. Continuous lines: observed data. Dashed lines: artificial anomaly starting at day 500.

To see this, an anomaly at the clinometer CL-1 of the north-west pylon is simulated as in Figure 12. It has the same transient timing as the above example on joints, but larger final sizes which are ± 1 the measurement standard deviation, that is $+0.03$ for channel A and and -0.007 for channel B. For this anomaly, the first and second level diagnostics of Figure 13 identifies the clinometers as the source of anomaly and the third level detectors are not reported here for brevity.

7 Conclusions

The large amount of data resulting from highly instrumented monitoring systems require appropriate tools for extracting useful information behind simple inspection and absolute thresholds. In this paper after a self-contained review of statistical surveillance an approach is presented for on-line analysis, early warnings and diagnostics.

The proposed methodology is capable of assessing field uncertainty and compensating for environmental biases. Moreover, modeling the correlations among measurements improves the efficiency in supervising the monitored system and in localizing the source of anomaly with a prefixed rate of false detections, especially for instruments strongly related to temperature.

The surveillance is based on a hierarchical multivariate detector which gives an easy to understand "statistical graphical dashboard" where, at top level, a single graph summarizes the whole monitoring system. In case of anomaly the top level detector gives a signal and subsequently the diagnostic system is able to localize the source of the anomaly.

As this approach is largely empirical, it requires historical data in order to be appropriately calibrated and validated. Nevertheless, even with a freshly installed monitoring system, a recursive estimation procedure may be implemented in order to start with a simpler model and improve iteratively the model estimates and its surveillance capability.

Last but not least, the data analysis process which is required for such an approach usually greatly improves the knowledge on the monitoring system and on structure health being monitored.
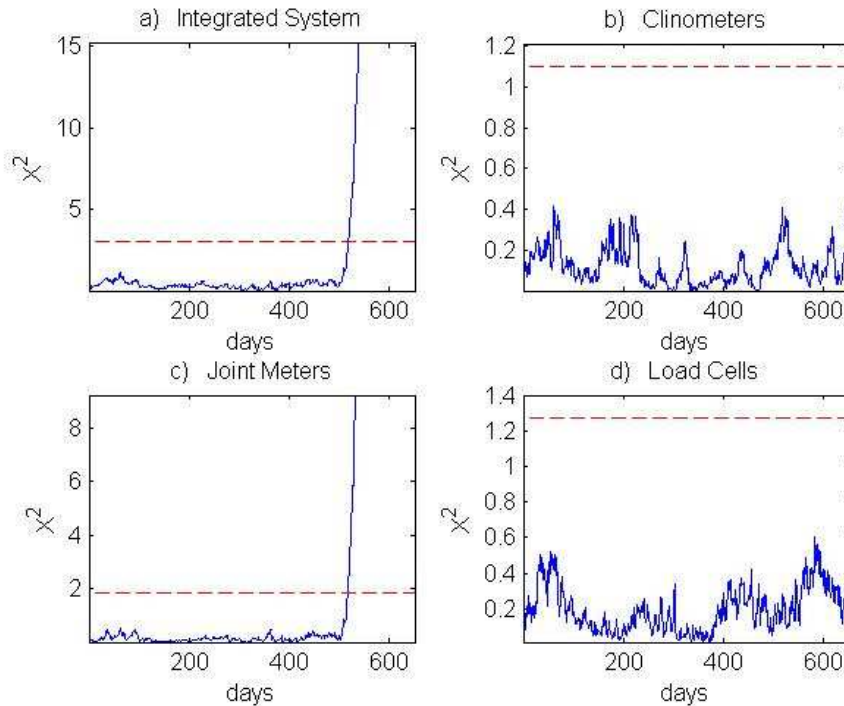
Figure 10: Joints anomaly. All panels: the horizontal dashed line is the threshold h. Panel a): The first level detector gives a signal on 515th day. Panels b), c), d): Second level detectors clearly identify the area of the anomaly.

References

[1] Aply, D.W. and Lee, H.C., 2005. Design of Exponentially Weighted Moving Average Control Charts for Autocorrelated Processes With Model Uncertainty. *Technometrics.* 45(3): 187-198.

[2] Basseville, M., Benveniste, A. Goursat, M. and Mevel, L., 2007. Subspace-Based Algorithms for Structural Identification, Damage Detection, and Sensor Data Fusion, *Journal on Advances in Signal Processing.* ID 69136.

[3] Basseville, M., Mevel, L., Goursat, M., 2004. Statistical model-based damage detection and localization: subspace-based residuals and damage-to-noise sensitivity ratios. *Journal of Sound and Vibration,* 275 (3-5): 769-794.

[4] Basseville, M., and Nikiforov, I.V., 1993. *Detection of Abrupt Changes,* Prentice Hall.

[5] Bayart, D., 2001. Walter Andrew Shewhart, *Statisticians of the Centuries* (ed. C. C. Heyde and E. Seneta) pp. 398-401. New York: Springer.

[6] Bersimis, S., Psarakis, S., Panaret, J., 2006. Multivariate Statistical Process Control Charts: An Overview. Qual. Reliab. Eng. Int. 23(5): 517 - 543
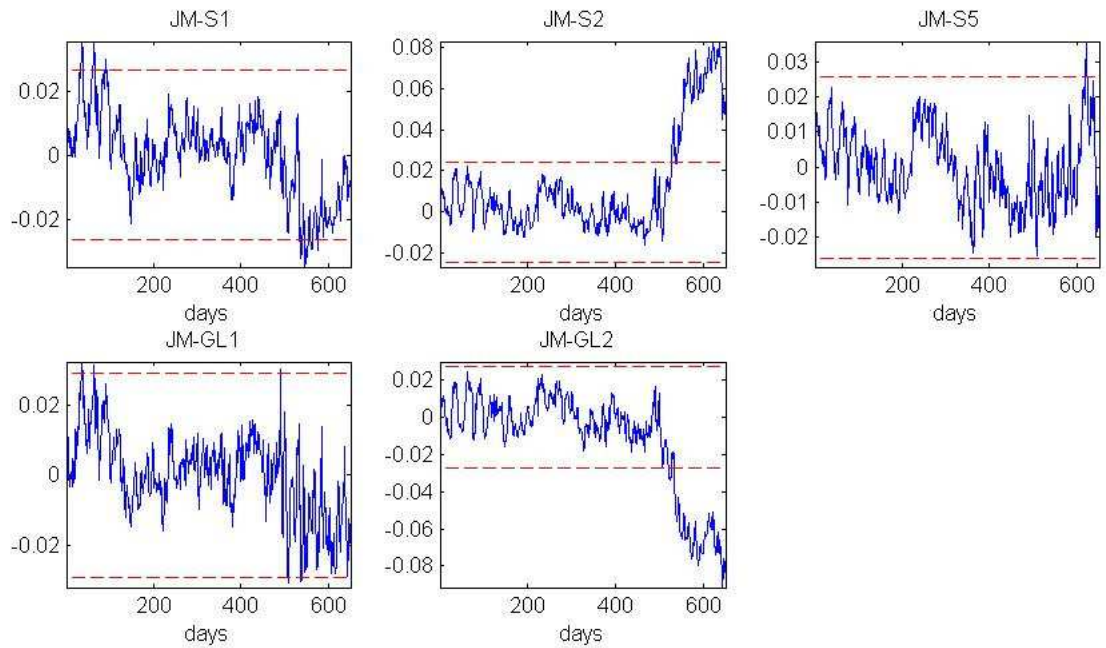
Figure 11: Third level detectors for jointmeters block based on $z_{j,t}$. All panels: The horizontal dashed lines are the thresholds $\pm\sqrt{h_j}$

[7] Biondini, F., Bontempi, F., Frangopol, D.M., Malerba, P.G., 2006a. Lifetime nonlinear analysis of concrete structures under uncertainty. In Cruz, Frangopol and Neves (eds). 2006. *Proceedings of the Third International Conference on Bridge, Maintenance, Safety and Management,* Taylor and Francis.

[8] Biondini, F., Frangopol, D.M., Malerba, P.G., 2006b. Time-variant Performance of the Certosa Cable-stayed Bridge. *Structural Engineering International.* 16(3): 235-244.

[9] Bruzzi, D., Fassò, A., Nicolis, O., Pezzetti, G., 2007. Statistical Analysis: a Tool for Understanding Monitoring Data. In DiMaggio, J. & Osborn, P. (Eds) FMGM 2007: *Proceedings of the 7th International Symposium on Field Measurements in Geomechanics*, ASCE.

[10] Carden, E.P. and Brownjohn, J.M.W., 2008. ARMA modelled time-series classification for structural health monitoring of civil infrastructure. *Mechanical Systems and Signal Processing.* 22(2): 295-314.

[11] Fassò, A. 1992. Localizing Ruptures in Block Stochastic Systems. J. Ital. Statist. Soc. 1(2).

[12] Fassò, A., Locatelli, S., 2007. Asymmetric Monitoring of Multivariate Data with Nonlinear Dynamics. *Advances in Statistical Analysis (AStA).* **91**:1, 23-27.

[13] Fassò, A. and Pezzetti, G., 2007. Statistical Methods for Monitoring Data Analysis. In DiMaggio, J. & Osborn, P. (Eds) FMGM 2007: Proceedings of the 7th International Symposium on Field Measurements in Geomechanics, ASCE.
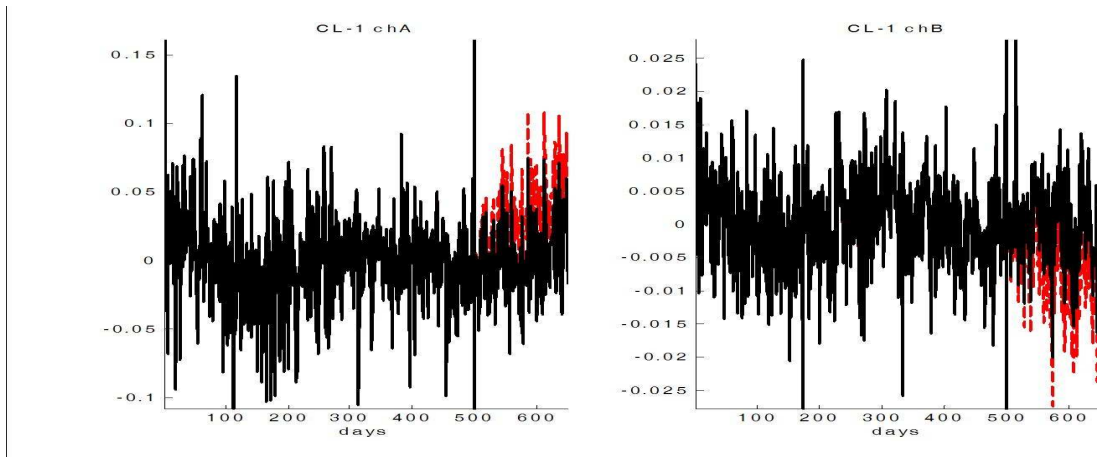
Figure 12: Artificial anomaly on the two channels clinometer CL-1 of the north-west pylon starting at day 500.

[14] Fuchs, C., Kenett, R.S., 1998. *Multivariate quality control. Theory and Applications*. Marcel Dekker, New York.

[15] Golosnoy, V., Schmid, W., 2007. EWMA control charts for monitoring changes in the optimal portfolio weights. *Sequential Analysis*, **26**:2, 195-224.

[16] Ljung, L. 1999. *System Identification, Theory for the User*, 2nd ed. Prentice Hall.

[17] Lowry, C. A., Woodall, W. H., Champ, C. W., and Rigdon, S. E., 1992. A Multivariate Exponentially Weighted Moving Average Chart, *Technometrics*, 34, 46-53.

[18] Montgomery, D.C. 2005. *Introduction to statistical quality control*, Fifth Edition. John Wiley and Sons, New York.

[19] Runger, G., Prabhu, S. 1996. A Markov chain model for the multivariate exponentially weighted moving averages control chart. *JASA*, **91,** 1701-1706.

[20] Shewhart, W.A., 1931. *Economic Control of Quality of Manufactured* Van Nostrand, New York.

[21] Ye, N., Borror, C., Zhang, Y., 2002. Ewma techniques for computer intrusion detection through anomalous changes in event intensity. *Quality and Reliability Engineering.* **18**, 443-451.

[22] Wah, T., 1971. Analysis of heat conduction in bridge slab, *Journal Acta Mechanica,* **11**:1-2, 9-26.

[23] Woodall, W., 2006. The Use of Control Charts in Health-Care and Public-Health Surveillance, *Journal of Quality Technology*, 2006, **38**:2, 89-104.
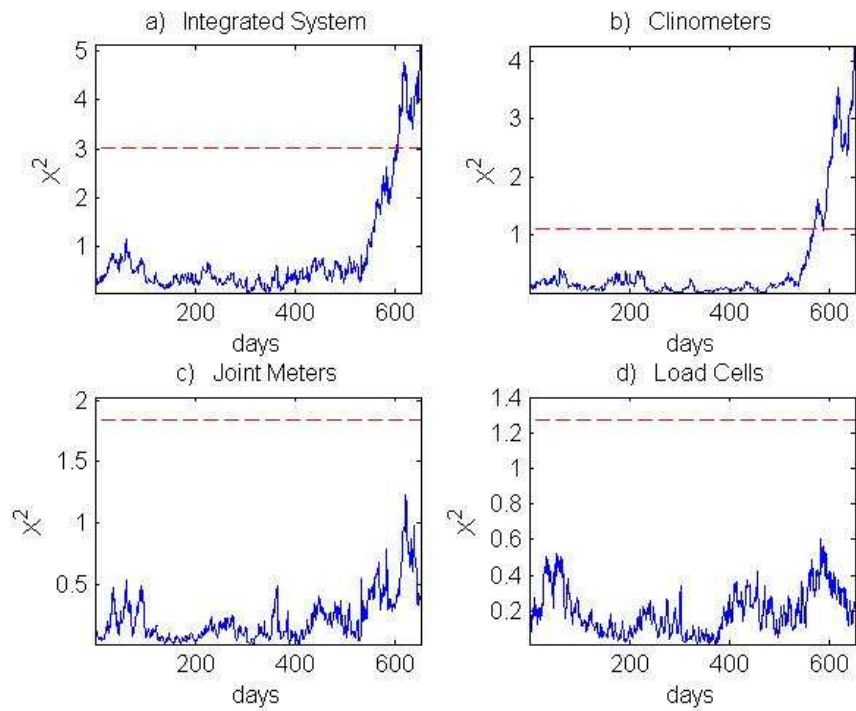
Figure 13: Clinometer anomaly. All panels: the horizontal dashed line is the threshold h. Panel a): The first level detector gives a signal on 601st day. Panels b), c), d): Second level detectors clearly identify the area of the anomaly.